Applied Clay Science 85 (2013) 25–30

Contents lists available at ScienceDirect

Applied Clay Science

journal homepage: www.elsevier.com/locate/clay

Research paper

High-pressure adsorption of methane on montmorillonite, kaolinite and illite

Dong Liu [a], Peng Yuan [a,*], Hongmei Liu [a,b], Tian Li [a,b], Daoyong Tan [a,b], Weiwei Yuan [a,b], Hongping He [a]

[a] CAS Key Laboratory of Mineralogy and Metallogeny, Guangzhou Institute of Geochemistry, Chinese Academy of Sciences, Guangzhou 510640, China
[b] University of Chinese Academy of Sciences, Beijing 100049, China

ARTICLE INFO

Article history:
Received 4 February 2013
Received in revised form 24 June 2013
Accepted 10 September 2013
Available online 2 October 2013

Keywords:
Methane (CH_4) adsorption
Clay minerals
Interlayer space
Montmorillonite
High pressure

ABSTRACT

Methane (CH_4) adsorption of Ca^{2+}-montmorillonite (Mt), kaolinite (Kaol) and illite (Il) at 60 °C and pressures up to 18.0 MPa was investigated, during which the adsorption capacity was evaluated by the Langmuir adsorption model. The influences of adsorbed water and the interlayer distance of the clay minerals on CH_4 adsorption were explored by using heated Mt products with different interlayer distances as the adsorbent. Mt, Kaol and Il showed high CH_4 adsorption capacities, and their maximum Langmuir adsorption capacities were Mt, 6.01 cm^3/g; Kaol, 3.88 cm^3/g; and Il, 2.22 cm^3/g, respectively. CH_4 was adsorbed only on the external surface of Kaol and Il; however, adsorption also occurred in the interlayer space of Mt, which had a larger interlayer distance than the size of a CH_4 molecule (0.38 nm). CH_4 adsorption in the interlayer space of Mt was supported by the lower CH_4 adsorption capacity of heated Mt products (with the interlayer distance <0.38 nm) than that of Mt at high pressures despite the higher external surface areas of the heated Mt samples. The entrance of CH_4 into the interlayer space of Mt occurred at low pressures, and more CH_4 molecules entered the interlayer space at high pressures. Moreover, the adsorbed water occupied the adsorption sites of the clay minerals and decreased the CH_4 adsorption capacity. These results indicate that clay minerals play a significant role in CH_4 adsorption of shale and indicate that the structure and surface properties of clay minerals are the important parameters for estimating the gas storage capacity of shale.

1. Introduction

Shale gas, which is derived from organic matters in shale and stored in shale deposits, is an important unconventional gas resource and has recently attracted attention for its promising exploitation (Chalmers and Bustin, 2008; Curtis, 2002; Jing et al., 2011; Loucks et al., 2009; Ross and Bustin, 2007, 2009; Zhang et al., 2012). Methane (CH_4) sourced from thermogenesis and/or biogenesis of organisms is the dominant component of shale gas (Hill et al., 2007; Strapoc et al., 2010; Zhang et al., 2012). The adsorption state is one of the most important forms of CH_4 in shale, and the content of adsorbed gases is up to 20–85% of total gases (Curtis, 2002; Jing et al., 2011; Montgomery et al., 2005). Therefore, investigating the adsorbed gases in shale is required not only to understand the reservoir and deliverability of shale gas but also to reduce the risks of exploration and to determine the economic feasibility of exploiting this resource (Chalmers and Bustin, 2008; Curtis, 2002; Ross and Bustin, 2007, 2008; Strapoc et al., 2010; Zhang et al., 2012).

Pressures and temperatures were proposed to be the main factors that influence CH_4 adsorption and CH_4 reservoir (Cheng and Huang, 2004; Cui et al., 2009; Lu et al., 1995; Ross and Bustin, 2009). The experimental evaluation showed that the CH_4 adsorption capacity of shale increases with the increment of pressure (Cheng and Huang, 2004; Loucks et al., 2009; Lu et al., 1995; Ross and Bustin, 2007, 2008), implying that the high pressures in the actual shale gas reservoir might result in a large CH_4 adsorption amount. In contrast, high reservoir temperatures are unfavorable with respect to CH_4 adsorption and decrease the adsorption capacity of shale (Ross and Bustin, 2008; Zhang et al., 2012).

Organic matters and clay minerals are the main components of shale. Abundant studies have focused on CH_4 adsorption in organic matters of shale, and the results have revealed a positive correlation between the organic content and the CH_4 adsorption capacity in raw shale samples (Cui et al., 2009; Lu et al., 1995). The mechanism of CH_4 adsorption in organic matters has been well documented, illustrating that the surface functional groups and micropores provided the adsorption sites for CH_4 (Loucks et al., 2009; Ross and Bustin, 2007, 2008, 2009; Zhang et al., 2012). The effects of the characteristics of organic matters on CH_4 adsorption, including the total organic carbon (TOC) content (Cluff and Dickerson, 1982; Harris et al., 1970), kerogen type (Zhang et al., 2012) and thermal maturity (Loucks et al., 2009), have also been investigated.

Compared with extensive studies of CH_4 adsorption in organic matters, less attention has been paid to CH_4 adsorption of clay minerals,

* Corresponding author at: Guangzhou Institute of Geochemistry, Chinese Academy of Sciences, Wushan, Guangzhou 510640, China. Tel./fax: +86 20 85290341.
E-mail address: yuanpeng@gig.ac.cn (P. Yuan).

0169-1317/$ – see front matter © 2013 Elsevier B.V. All rights reserved.
http://dx.doi.org/10.1016/j.clay.2013.09.009

although clay minerals are the important component of shale. This lack of research may be because it is assumed that clay minerals have higher hydrophilicity and lower porosity than organic matters; consequently, it is expected that clay minerals would encounter difficulty in the adsorption of CH_4. However, Schettler and Parmoly proposed that clay minerals played an important role in CH_4 adsorption in their study of CH_4 adsorption on shale samples from Appalachian basin shales, which had low kerogen contents (Schettler and Parmoly, 1990). Since then, CH_4 adsorption on clay minerals has been investigated by others (Cheng and Huang, 2004; Lu et al., 1995; Ross and Bustin, 2009). In experimental measurements of CH_4 adsorption on clay minerals at various temperatures and low pressures, clay minerals were found to provide adsorption sites and space for CH_4 storage (Cheng and Huang, 2004; Lu et al., 1995; Ross and Bustin, 2009). The maximum CH_4 adsorption capacity of pure illite at 37.8 °C and ≤8.0 MPa was higher than that of shale samples obtained from wells of Michigan, West Virginia and Kentucky, USA (Lu et al., 1995). Unexpectedly, the evaluation of the CH_4 adsorption capacity on montmorillonite and kaolinite showed higher CH_4 uptake by kaolinite than Na^+-saturated montmorillonite at low pressures (≤0.3 MPa) (Cheng and Huang, 2004). Ross and Bustin further found that at low pressures (6.0 MPa), the CH_4 adsorption capacities of illite (0.4 cm^3/g) and montmorillonite (0.6 cm^3/g) were lower than that of kaolinite (0.7 cm^3/g) on a moisture-equilibrated basis, but were significantly higher (montmorillonite: 2.9 cm^3/g and illite: 2.1 cm^3/g) than that of kaolinite (0.7 cm^3/g) under dry conditions (Ross and Bustin, 2009).

Although the abovementioned studies investigated the CH_4 absorption capacity of clay minerals, unfortunately, the CH_4 adsorption mechanisms, including CH_4 adsorption sites and influencing factors, remain unclear. One of the major reasons for this lack of progress is the coexistence of organic matters during adsorption measurements; thus, the effects of organic matter could not be avoided (Ross and Bustin, 2009), which prevented the adsorption mechanism of clay minerals from being exclusively addressed. Another major reason is that the pressure, which is an important evaluation parameter of the CH_4 adsorption capacity, ranged less extensively (≤8.0 MPa) in the previous studies (Cheng and Huang, 2004; Crosdale et al., 1998; Lu et al., 1995; Ross and Bustin, 2007; Sun et al., 2009). Further, such pressure values are not representative of the actual reservoir pressures of shale gas (Chalmers and Bustin, 2008). Moreover, the clay mineral samples were inappropriately selected for the evaluation of CH_4 adsorption. For example, clay minerals with a small interlayer distance, such as Na^+-saturated montmorillonite, were used to represent the group of swelling clay minerals (Cheng and Huang, 2004; Ross and Bustin, 2009). However, the interlayer distance of Na^+-saturated montmorillonite was approximately 0.1–0.3 nm (Aylmore et al., 1970; Hellerkallai, 2006; Michot and Villieras, 2006), which is smaller than the size of a CH_4 molecule (approximately 0.38 nm) (Suzuki et al., 1995; Volzone and Ortiga, 2004). Therefore, CH_4 adsorption on montmorillonite with a large interlayer distance (such as montmorillonite with calcium ions as the main interlayer cation species: Ca^{2+}-montmorillonite, with an interlayer distance > 0.4 nm) was neglected. Thus, the results were also not representative from this perspective, which has resulted in a misunderstanding of the CH_4 adsorption sites of clay minerals. Swelling clay minerals with a large interlayer distance, such as Ca^{2+}-montmorillonite, should be selected for a complementary investigation to estimate the influence of the interlayer distance on CH_4 adsorption. However, to the best of our knowledge, very few studies have been reported on this topic.

In this study, CH_4 was adsorbed onto Ca^{2+}-montmorillonite, kaolinite and illite at high hydrostatic pressures (up to 18.0 MPa), which were applied to simulate the reservoir pressures of shale gas. The main objectives of this study were to explore i) the CH_4 adsorption capacity of various clay minerals and ii) the corresponding adsorption mechanism, such as the adsorption sites and influencing factors. Heating was carried out to change the interlayer distance of Ca^{2+}-montmorillonite to investigate CH_4 adsorption in the interlayer space, and the structure–adsorption correlation of clay minerals was examined by combining thermogravimetric (TG) analysis, X-ray diffraction (XRD) and N_2 adsorption–desorption methods.

2. Materials and methods

Montmorillonite, kaolinite and illite were sourced from Inner Mongolia, Guangdong, and Hebei, China, respectively. A purification method of hand picking followed by repeated sedimentation was applied to remove impurities. The chemical compositions of the purified montmorillonite, kaolinite and illite (denoted as Mt, Kaol and Il, respectively) are showed in Table 1. The structural formula of Mt is $Ca_{0.168}\ Na_{0.025}\ K_{0.013}\ (Si_{3.806}\ Al_{0.194})\ (Al_{1.172}\ Fe_{0.270}\ Mg_{0.367}\ Ti_{0.010}\ Mn_{0.002})\ O_{10}\ (OH_2)\cdot nH_2O$, and the CEC value is 110.5 cmol (+) kg^{-1}. The structural formula of Il is $Ca_{0.010}\ Na_{0.028}\ K_{0.572}\ (Si_{3.030}\ Al_{0.970})\ (Al_{1.570}\ Fe_{0.084}\ Mg_{0.032}\ Ti_{0.023}\ Mn_{0.002})\ O_{10}\ (OH_2)\cdot nH_2O$, and the CEC value is 3.9 cmol (+) kg^{-1}. The structural formula of Kaol is $(Si_2)^{IV}\ (Al_2)^{VI}\ O_5\ (OH)_4$, and the CEC value is near to zero.

Heating treatment of Mt was performed in a programmed temperature-controlled muffle oven at 200, 400 and 600 °C for 3 h each. The heated samples were then ground by hand for 1 min in an agate mortar and denoted as Mt-200, Mt-400 and Mt-600. To avoid the re-adsorption of water, these samples were placed in a desiccator in which allochroic silica gel had been loaded, and vacuumization was subsequently performed to maintain a dry environment.

XRD patterns were recorded on a Bruker D8 Advance diffractometer with a Ni filter and Cu K alpha radiation ($\lambda = 0.154$ nm) using a generator voltage of 40 kV and generator current of 40 mA. A scan rate of 1° (2θ)/min was used to record the XRD patterns.

N_2 adsorption–desorption isotherms were measured on a Micromeritics ASAP 2020 system (Micromeritics Co., Norcross, USA) at the temperature of liquid nitrogen. Samples were outgassed at 60 °C, which corresponded with the CH_4 adsorption temperature, for 12 h at the degas port and then transferred to the analysis port for 6 h of further degassing below a relative pressure of 0.01 before being measured. The specific surface area, S_{BET}, was calculated using the multiple-point Brunauer–Emmett–Teller (BET) method.

The CH_4 adsorption measurement of clay minerals was performed on an automated Sieverts' apparatus (PCT-Pro-E&E from Setaram Instrumentation) over a pressure range of 0–18.0 MPa and at 60 °C with an error (Δt) of ±0.2 °C. Helium gas (He, 99.999 mass %) was used as the calibration gas, and nitrogen gas (N_2, 99.999 mass %) was used as the carrier gas. The Langmuir equation, a model related to the coverage or adsorption of gas molecules on a solid surface at a fixed temperature, was used to evaluate the CH_4 adsorption capacity of clay minerals. This model describes the monolayer adsorption state of CH_4 on the clay minerals, which offers many nearly energetically homogenous adsorption sites at various pressures (Gregg and Sing, 1967; Keller and Staudt, 2004; Langmuir, 1918); the model is expressed as $V = V_L P/(P_L + P)$, where V (cm^3/g) is the volume of absorbed gas at pressure P (MPa), V_L (cm^3/g) is the Langmuir maximum adsorption capacity, P (MPa) is the gas pressure and P_L (MPa) is the Langmuir pressure.

Table 1
The chemical compositions of Mt, Kaol and Il.

Samples	Chemical compositions (% mass)										
	SiO_2	Al_2O_3	Fe_2O_3	CaO	MgO	K_2O	Na_2O	MnO	TiO_2	P_2O_5	L.O.I.
Mt	58.16	16.95	5.26	2.29	3.57	0.15	0.19	0.03	0.20	0.08	13.25
Kaol	46.66	38.20	0.69	–	0.10	0.37	0.04	–	0.36	0.03	13.60
Il	50.66	32.77	1.69	0.14	0.32	6.80	0.22	0.04	0.47	0.16	6.78

– represents trace, and L.O.I. denotes loss on ignition.

3. Results

3.1. XRD of Mt, Kaol, Il and heated products of Mt

The XRD patterns of Mt, Kaol and Il illustrate the main phases of highly ordered crystalline of montmorillonite, kaolinite and illite (Fig. 1a). The (001) characteristic diffraction reflections of Mt, Kaol and Il appear at approximately 6°, 9° and 13° (2θ) with d_{001} values of 1.47, 1.00 and 0.72 nm, respectively. The interlayer distances of Mt and Il were obtained by subtracting the thickness of the structural layer unit (tetrahedron–octahedron–tetrahedron, TOT, approximately 0.96 nm) from the basal spacing (d_{001} value), yielding values of approximately 0.51 and 0.04 nm, respectively (Table 2). Accordingly, the interlayer distance of Kaol was obtained by subtracting 0.71 nm (the thickness of the TO layer) from the basal spacing, resulting in a measurement of approximately 0.01 nm. Quartz impurities were also found in the three clay minerals, with weak reflections at approximately 22° and 27° (Fig. 1a). The contents (mass %) of quartz were semi-quantitatively determined as 3% in Mt, 4% in Kaol and 5% in Il.

The interlayer distance of Mt products was significantly affected by heating. The interlayer distance of the Mt samples decreased with the increasing temperature (Table 2) due to desorption of the interlayer water and dehydroxylation (He et al., 2006; Heller-kallai, 2006). This result was consistent with the TG analysis (see Supplementary data, Fig. S1). The interlayer distance of Mt after heating at 200 and 400 °C decreased from approximately 0.51 to 0.48 nm (Mt-200) and 0.01 nm (Mt-400). The interlayer distance of Mt-600 was near zero (Table 2) because the interlayer space had collapsed after the complete dehydration and removal of the partial hydroxyl groups.

3.2. CH_4 adsorption

3.2.1. CH_4 adsorption of Mt, Kaol and Il

The CH_4 adsorption isotherms of Mt, Kaol and Il show that the adsorption capacity increased with the increasing pressure at low pressures and remained nearly constant at high pressures (Fig. 2a). The adsorption data were fitted to the Langmuir model ($R^2 > 0.96$) (Fig. 2a and Table 2, Sun et al., 2009; Zhang et al., 2012). It is noteworthy that the effect of quartz on CH_4 adsorption of the clay minerals was negligible because there were very few quartz impurities and quartz had a very low adsorption capacity for CH_4 (V_L: 0.55 cm^3/g, see Supplementary data, Fig. S2).

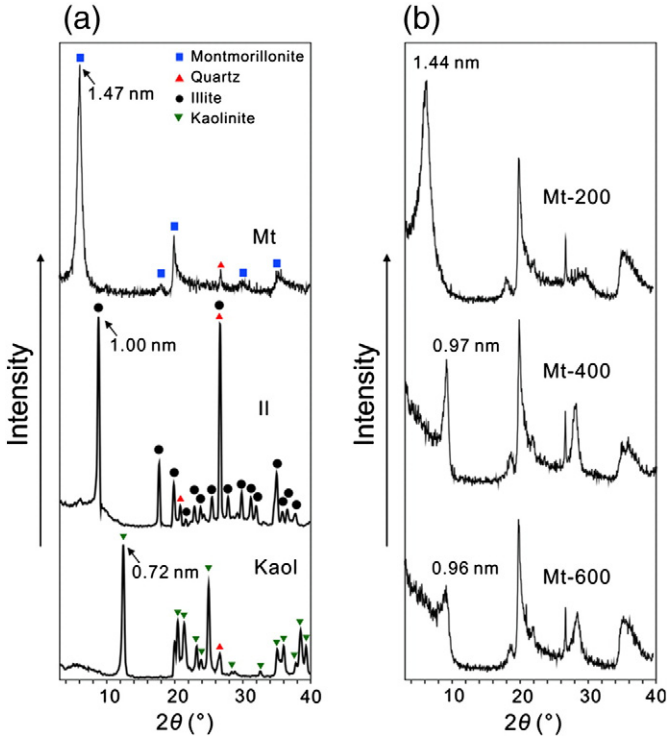

Fig. 1. XRD patterns of (a) Mt, Il and Kaol; (b) heated products of Mt.

Table 2
Langmuir equation parameters for CH_4 adsorption, surface areas and the interlayer distance of various absorbents.

Sample	V_L (cm^3/g STP)	P_L (MPa)	R^2	S_{BET} (m^2/g)	Interlayer distance (nm)
Mt	6.01	3.5	0.9787	56.5	~0.51
Mt-200	7.61	1.9	0.9574	74.5	~0.48
Mt-400	4.83	1.2	0.9649	65.7	~0.01
Mt-600	4.76	2.4	0.9879	56.6	~0
Kaol	3.88	3.0	0.9671	15.7	~0.01
Il	2.22	3.1	0.9958	11.2	~0.04

The V_L values for the three samples followed the order of Mt (6.01 cm^3/g) > Kaol (3.88 cm^3/g) > Il (2.22 cm^3/g) (Table 2). Mt showed the largest CH_4 adsorption capacity, indicating that it contributes more to CH_4 adsorption of shale than do Kaol and Il. The Langmuir pressure (P_L) represents the pressure at which the gas adsorption capacity equals one-half of the maximum gas adsorption capacity. P_L values are typically used to evaluate the CH_4 affinity of absorbents and the feasibility of gas desorption under reservoir pressures; lower P_L values indicated that CH_4 adsorption occurs more readily and that desorption is more difficult to achieve (Ross and Bustin, 2007; Zhang et al., 2012). As showed in Table 2, the P_L values of Kaol and Il had very slight differences, exhibiting similar CH_4 affinities; additionally, the fact that the values were smaller than that of Mt indicated that CH_4 was readily adsorbed on Kaol and Il at low pressures, which might be attributed to the lower contents of adsorbed water on the surfaces of Kaol and Il.

3.2.2. CH_4 adsorption of the heated Mt products

The adsorption data of the heated Mt samples were fitted to the Langmuir model ($R^2 > 0.95$, Table 2), similarly to those of the raw clay minerals (Mt, Kaol and Il). The CH_4 adsorption capacity of Mt varied with heating. The V_L value (7.61 cm^3/g) of Mt-200 was the largest among all the Mt samples (Table 2). The V_L values for Mt-400 and Mt-600 were both similar and smaller than that of Mt. However, the order of the CH_4 adsorption capacity for Mt and its heated products varied with the pressure. At low pressures ($P < 2.4$ MPa), the CH_4 adsorption capacity followed the order of Mt-200 > Mt-400 > Mt-600 > Mt (Fig. 2b), which exhibited the same order as the S_{BET} values of Mt and its heated products; in the pressure range of $2.4 < P < 7.2$ MPa, the order was Mt-200 > Mt-400 > Mt > Mt-600; When $P > 7.2$ MPa, the order was Mt-200 > Mt > Mt-400 > Mt-600. The CH_4 adsorption capacity of Mt was equal to the values obtained for Mt-200 at 2.4 MPa and Mt-400 at 7.2 MPa. The smallest P_L value (1.2 MPa) was observed in Mt-400, which suggests that CH_4 was more readily adsorbed on Mt-400 than the other Mt samples.

4. Discussion

CH_4 and N_2 have often been used as probe molecules to evaluate the gas adsorption capacity and porosity of Mt and its derivatives (Bakandritsos et al., 2005; Barrer and Reay, 1957; Maes et al., 1997; Volzone and Ortiga, 2004). The estimation parameters of Mt based on N_2 and CH_4 adsorption are comparable (Volzone and Ortiga, 2004) because i) both CH_4 and N_2 are nonpolar molecules and are physically adsorbed on Mt, and ii) the kinetic diameter of CH_4 (0.38 nm) is similar to that of N_2 (0.35 nm). Considering that the mechanism of N_2 adsorption on Mt, such as the adsorption sites and influencing factors, has been well investigated (Aylmore et al., 1970; Kaufhold et al., 2010; Maes

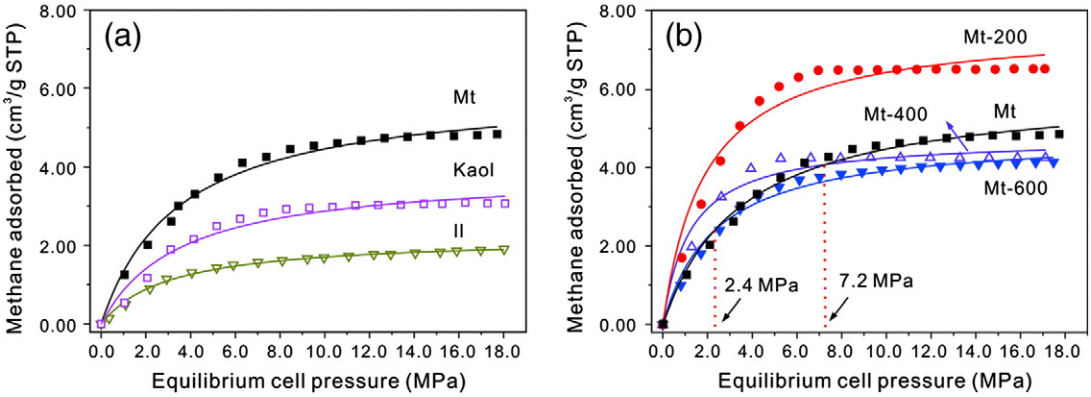

Fig. 2. The adsorption isotherms of CH_4 on (a) Mt, Kaol and Il; (b) Mt and its heated products.

et al., 1997; Michot and Villieras, 2006; Volzone and Ortiga, 2004), the N_2 adsorption data and parameters of clay minerals are herein referenced in the evaluation of the adsorption property of CH_4.

N_2 adsorption has typically been performed to obtain the surface area of clay minerals (Aylmore et al., 1970; Barrer and Reay, 1957; Kaufhold et al., 2010; Maes et al., 1997; Michot and Villieras, 2006). The obtained S_{BET} values varied according to the measurement conditions and samples in previous reports. This is because N_2 adsorption on clay minerals was affected by adsorbed water and the structure of the clay minerals (Aylmore et al., 1970; Michot and Villieras, 2006). For the former, the water was adsorbed on the hydrophilic surface of clay minerals and occupied the most adsorption sites and space, which left little space for N_2 molecules. For the latter, the interlayer distance was proposed to determine whether N_2 molecules could enter the interlayer space of clay minerals. It is possible that N_2 entered the interlayer space of clay minerals only when the interlayer distance was larger than the molecular size of N_2 (0.35 nm) (Kaufhold et al., 2010; Michot and Villieras, 2006). This proposed explanation agrees with our results, indicating that the N_2 adsorption capacity (the adsorption capacity when $P/P_0 \leq 0.1$; Hernaandez et al., 2000; Pierotti and Rouquerol, 1985) in micropores which was primarily derived from the interlayer space was low when the adsorbed water was not removed, although Mt is known to contain abundant micropores. Very few micropores were detected in Kaol and Il due to their smaller interlayer distances relative to the size of the N_2 molecule (see Supplementary data, Fig. S3); thus, the S_{BET} values of Kaol and Il were proposed to represent their external surface areas.

The interlayer distance of Mt decreased with the increasing temperature, as demonstrated by the decreasing d_{001} value (Fig. 1), due to the removal of interlayer water and hydroxyl groups (see Supplementary data, Fig. S1). After heating to 400 °C, almost all of the interlayer adsorbed water was removed, and dehydroxylation occurred at 600 °C (see Supplementary data, Fig. S1), during which the layered structure of Mt was destroyed and the interlayer space gradually disappeared (Fig. 1). As mentioned above, heating decreased not only the content of adsorbed water of Mt, but also the interlayer distance. Therefore, heating changed the S_{BET} value of the Mt samples. After heating at 200, 400 and 600 °C, both the adsorbed water and interlayer distance of Mt decreased, and the S_{BET} values increased (Table 2). These trends occurred due to the increased availability of CH_4 adsorption sites following the removal of adsorbed water. Compared with Mt-200, the S_{BET} values of Mt-400 and Mt-600 were smaller, although more adsorbed water was removed after heating to 400 and 600 °C. This observation can be explained by the decrease in the interlayer distance to a size smaller than a N_2 size (Table 2), which prevented N_2 from entering the interlayer space. Therefore, the S_{BET} values of Mt-400 and Mt-600 reflect only their external surface areas. In light of the fact that the layered structure was retained in Mt-400 but destroyed in Mt-600 by heating (Noyan et al., 2006), the measured S_{BET} of Mt-400 could accurately represent the external surface area of Mt without the interference of adsorbed water.

CH_4 adsorption was similar to N_2 adsorption on layered clay minerals because of the comparable size and adsorption properties of N_2 and CH_4. CH_4 adsorption was also affected by adsorbed water and the interlayer distance of clay minerals. Similar to N_2, CH_4 could not be adsorbed in the interlayer space of Kaol and Il and was adsorbed only on the external surface. Accordingly, the adsorption capacity of Kaol and Il depended on the external surface area (S_{BET} of Kaol and Il). Compared with Il, Kaol had a higher external surface area (Table 2) and less adsorbed water (see Supplementary data, Fig. S1), which should have led to a higher CH_4 adsorption capacity. This assumption was supported by the results of CH_4 adsorption (Table 2). Mt had a larger CH_4 adsorption capacity (Table 2) and higher P_L value than either Kaol or Il, and these findings were attributed to the larger surface area and higher content of adsorbed water of Mt, respectively.

To explore the influence of adsorbed water and whether the CH_4 molecules were adsorbed in the interlayer space, Mt derivatives were used as CH_4 absorbents. These derivatives were obtained by heating at various temperatures and had different interlayer distances as a result (Table 2). After heating to 200 °C, the adsorbed water on the external surface of Mt had been removed (see Supplementary data, Fig. S1); therefore, the CH_4 adsorption capacity of Mt-200 was higher than that of Mt (Table 2). This result can be explained by the occupation of the adsorption sites of CH_4 by the water molecules present on the clay minerals, which decreased the CH_4 adsorption capacity; this finding is in agreement with the results that the CH_4 adsorption capacity decreased with the increasing moisture content (Krooss et al., 2002; Ross and Bustin, 2007, 2008, 2009).

At pressures > 2.4 MPa, Mt had a higher CH_4 adsorption capacity than Mt-600. However, it was expected that Mt-600 would have a higher adsorption capacity than Mt because the adsorbed water of Mt-600 had been removed (see Supplementary data, Fig. S1), resulting in a higher surface area (S_{BET}) (Table 2), which generally favors CH_4 adsorption. Similarly, at pressures > 7.2 MPa, Mt had a higher adsorption capacity than Mt-400, although Mt-400 had less adsorbed water. These interesting results demonstrate that some CH_4 molecules entered the interlayer space of Mt under the experimental conditions, indicating that CH_4 was adsorbed not only on the external surface but also in the interlayer space with a large interlayer distance. Moreover, the V_L values of Mt and Mt-200 were higher than those of Mt-400 and Mt-600, which was attributed to the fact that Mt-200 had a larger interlayer distance than a CH_4 size, whereas the interlayer distances of Mt-400 and Mt-600 were smaller. It is noteworthy that the CH_4 adsorption capacity of Na^+-saturated Mt (Cheng and Huang, 2004; Ross and Bustin, 2009) was lower than that of Ca^{2+}-Mt, possibly because the interlayer distance of Na^+-saturated Mt is smaller than the CH_4 molecule.

When $P = 2.4$ MPa, the CH_4 adsorption capacity of Mt was equal to that of Mt-600. In view of the fact that Mt had a smaller S_{BET} value than Mt-600, CH_4 molecules were able to enter the interlayer space of Mt at or even below this pressure. Similarly, the CH_4 adsorption capacities of Mt and Mt-400 were the same at 7.2 MPa. A pressure of 2.4 MPa, at which CH_4 adsorption occurred in the interlayer space of Mt, is lower than the actual reservoir pressure (from 2.9 to 17.6 MPa) of the Lower Cretaceous shales in northeastern British Columbia (Chalmers and Bustin, 2008). This result indicates that under actual reservoir conditions, CH_4 is very likely to be adsorbed in the interlayer space of Mt. To the best of our knowledge, this study is the first to propose that CH_4 adsorption occurs in the interlayer space of clay minerals with large interlayer distances.

Therefore, as showed in Fig. 2b, the various adsorption capacity orders of Mt samples at different pressures can be interpreted as follows. At low pressures ($P < 2.4$ MPa), the sequence of the CH_4 adsorption capacity followed the order of S_{BET} (Mt-200 > Mt-400 > Mt-600 > Mt). With increasing pressure, more CH_4 molecules entered the interlayer space of Mt and Mt-200, however, CH_4 molecules were not able to enter the interlayer space of Mt-400 and Mt-600, resulting in the adsorption capacity order of Mt-200 > Mt > Mt-400 > Mt-600 at pressures > 7.2 MPa. Moreover, Mt-200 had little adsorbed water on its external surface, and its interlayer distance was > 0.38 nm (Table 2), which resulted in the highest CH_4 adsorption capacity among all the samples.

Compared with most raw shale samples (including organic rich-shale samples), Mt had the higher CH_4 adsorption capacity (Langmuir maximum adsorption capacity: 6.01 cm^3/g) (Chalmers and Bustin, 2008; Ross and Bustin, 2007, 2008, 2009; Zhang et al., 2012). For example, the CH_4 adsorption capacity of organic-rich (TOC content ≤ 11.8, mass %) Lower Jurassic Gordondale Member shales was up to 2.01 cm^3/g under simulated reservoir conditions (at pressures ≤ 9.0 MPa and a temperature of 30 °C) (Ross and Bustin, 2007), and the values of some shale samples (TOC content ranged from 6.6 to 20.7, mass %) sourced from the Barnett Shale well were only 0.12–0.24 mmol/g (2.69–5.38 cm^3/g) obtained at pressures ≤ 15.0 MPa (Zhang et al., 2012). Moreover, it is noteworthy that the CH_4 adsorption capacity of some shale samples without or with very small fractions of Mt was low, although these samples contained abundant content of other clay minerals, such as Il and Kaol. For example, the Langmuir maximum adsorption capacity of CH_4 in clay-rich shale samples (total clay content: 77, mass %, and primarily composed of Il, chlorite and Kaol) was 0.65 cm^3/g at reservoir pressures (from 2.9 to 17.6 MPa) (Chalmers and Bustin, 2008), and the value in a shale sample derived from Besa River (total clay content: 88.3, mass %, primarily composed of Il and Kaol) was only <0.01 cm^3/g at the reservoir temperature of 154.9 °C and pressures up to 40.0 MPa (Ross and Bustin, 2008). These results are in good agreement with our results that Mt demonstrated significantly more adsorption capacity than other primary shale clay minerals, such as Kaol and Il, indicating that Mt plays an important role in the adsorption and storage of CH_4 in shale.

The CH_4 adsorption capacity of Mt was less than that of organic matters in shale samples obtained from Barnett Shale (Langmuir maximum adsorption capacity ≥ 1.21 mmol/g (27.10 cm^3/g), at pressures ≤ 16.0 MPa; Zhang et al., 2012), showing that organic matters contribute much more to CH_4 adsorption than clay minerals. The high CH_4 adsorption capacity of organic matters was attributed to the abundance of adsorption sites, such as surface functional groups on which CH_4 was adsorbed mainly by hydrogen bonds and micropores (Loucks et al., 2009; Ross and Bustin, 2007, 2008, 2009; Zhang et al., 2012). Kaol and Il exhibited lower CH_4 adsorption capacities than organic-rich shale samples (Ross and Bustin, 2007; Zhang et al., 2012).

Similar to our results, the CH_4 adsorption capacity of clay minerals, as obtained in previous studies, increased with the increasing pressure, and the adsorption isotherms were fitted to the Langmuir model (Lu et al., 1995; Ross and Bustin, 2009). It is noteworthy that the order of the adsorption capacity of clay minerals obtained by Ross and Bustin (2009) was different with ours, and showed Il > Mt. The difference is mainly due to the variation among the Mt samples. In the report, Na^+-saturated Mt with a low surface area (24.7 m^2/g) was used as the adsorbent. Due to the smaller interlayer distance of Na^+-saturated Mt relative to the size of the CH_4 molecule, CH_4 could only be adsorbed on the external surface of Na^+-saturated Mt, and thus the adsorption capacity of this mineral was smaller than that of Ca^{2+}-Mt used in our experiment. Moreover, the Il sample used in the report had a larger external surface area (30.0 m^2/g) than that of Na^+-saturated Mt. Therefore, for these specific clay minerals it is reasonable that the CH_4 adsorption capacity of Il was higher than that of Na^+-saturated Mt because CH_4 adsorption only occurred on the external surface of the Il and Na^+-Mt. Based on this knowledge, the results of CH_4 adsorption evaluation on clay minerals presented in previous reports and in this study cannot be generalized to all cases due to the variations among the properties of a given type of clay mineral. Examples include the surface area of the mineral. However, our study focused on the influence of the interlayer distance before and after heating on the CH_4 adsorption and was not concerned with a comparison of the CH_4 adsorption capacities of various samples of one clay mineral with different origins. Moreover, the changes in the interlayer distance by heating for one clay mineral (such as Ca^{2+}-Mt) are not expected to be influenced by its origin due to the common basic structure possessed among samples of one clay mineral type. Therefore, it is more likely that the differences of the CH_4 adsorption capacity resulted from changes to the interlayer distances of Mt.

Moreover, as reported in some literatures (Lu et al., 1995; Ross and Bustin, 2007, 2009), low pressures were selected for the CH_4 adsorption evaluation. In these cases, the adsorption of CH_4 on clay minerals had not reached saturation levels, even at the highest pressure, and the adsorption capacity still showed an increasing trend according to the adsorption isotherms presented under the experimental conditions. Based on these results, the obtained Langmuir maximum adsorption capacity differed compared to that obtained by saturated adsorption. For example, in our study, the Langmuir maximum adsorption capacity of Mt obtained from the adsorption capacity at a pressure range from 0 to 8.0 MPa is 7.42 cm^3/g, which is higher than that obtained at pressures ranging from 0 to 18.0 MPa (6.01 cm^3/g); this result demonstrates an overestimation of the CH_4 adsorption capacity. Therefore, high pressures based on actual reservoir pressures should be used to accurately evaluate the CH_4 adsorption capacity of clay minerals.

5. Conclusions

In this study, the respective CH_4 adsorption capacity and mechanism of Mt, Kaol and Il at 60°C and pressures up to 18.0 MPa were investigated. Mt, Kaol and Il showed different CH_4 adsorption capacities, and the Langmuir maximum adsorption capacities were 6.01, 3.88 and 2.22 cm^3/g, respectively, indicating the high contribution of clay minerals to CH_4 adsorption in shale. Both adsorbed water and the interlayer distance of clay minerals affected CH_4 adsorption. Adsorbed water can occupy the adsorption sites, leaving little space for CH_4 adsorption. Kaol and Il had the lower contents of adsorbed water than Mt and showed more readily to adsorb CH_4. Mt was able to adsorb the CH_4 molecules in its interlayer space because the interlayer distance of this mineral was larger than the size of the CH_4 molecule. The entrance of CH_4 into the interlayer space of Mt occurred at low pressures, and more CH_4 molecules entered the interlayer space at high pressures.

Acknowledgments

This study was financially supported by the National Basic Research Program of China (Grant No. 2012CB214704-01), the National Natural Science Foundation of China (Grant No. 41272059), and the National S&T Major Project of China (Grant No. 2011ZX05008-002-21). This is a contribution (No. IS-1740) from GIGCAS.

Appendix A. Supplementary data

Supplementary data to this article can be found online at http://dx.doi.org/10.1016/j.clay.2013.09.009.

References

Aylmore, L., Sills, I., Quirk, J., 1970. Surface area of homoionic illite and montmorillonite clay minerals as measured by the sorption of nitrogen and carbon dioxide. Clay. Clay. Miner. 18, 91–96.

Bakandritsos, A., Kouvelos, E., Steriotis, T., Petridis, D., 2005. Aqueous and gaseous adsorption from montmorillonite-carbon composites and from derived carbons. Langmuir 21 (6), 2349–2355.

Barrer, R.M., Reay, J.S.S., 1957. Sorption and intercalation by methyl-ammonium montmorillonites. Trans. Faraday Soc. 53, 1253–1261.

Chalmers, G.R.L., Bustin, R.M., 2008. Lower Cretaceous gas shales in northeastern British Columbia, Part II: evaluation of regional potential gas resources. Bull. Can. Petrol. Geol. 56 (1), 22–61.

Cheng, A.L., Huang, W.L., 2004. Selective adsorption of hydrocarbon gases on clays and organic matter. Org. Geochem. 35 (4), 413–423.

Cluff, R., Dickerson, D., 1982. Natural gas potential of the New Albany Shale group (Devonian–Mississippian) in Southeastern Illinois. Old SPE J. 22 (2), 291–300.

Crosdale, P.J., Beamish, B.B., Valix, M., 1998. Coalbed methane sorption related to coal composition. Int. J. Coal Geol. 35 (1–4), 147–158.

Cui, X., Bustin, A., Bustin, R.M., 2009. Measurements of gas permeability and diffusivity of tight reservoir rocks: different approaches and their applications. Geofluids 9 (3), 208–223.

Curtis, J.B., 2002. Fractured shale-gas systems. AAPG Bull. 86 (11), 1921–1938.

Gregg, S., Sing, K., 1967. Adsorption, Surface Area, and Porosity. Academic Press, Inc., Ltd., London.

Harris, L.D., De Witt JR, W., Colton, G., 1970. What are possible stratigraphic controls for gas fields in eastern black shale. Oil Gas J. 76 (14), 162–165.

He, H., Yang, D., Yuan, P., Shen, W., Frost, R., 2006. A novel organoclay with antibacterial activity prepared from montmorillonite and Chlorhexidini Acetas. J. Colloid Interface Sci 297 (1), 235–243.

Heller-kallai, L., 2006. Thermally modified clay minerals. In: Bergaya, F., Theng, B.K.G., Lagaly, G. (Eds.), Handbook of Clay Science. Dev. Clay Sci., vol. 1. Elsevier, Amsterdam, pp. 289–296.

Hernaandez, M., Corona, L., Rojas, F., 2000. Adsorption characteristics of natural erionite, clinoptilolite and mordenite zeolites from Mexico. Adsorption 6 (1), 33–45.

Hill, R.J., Jarvie, D.M., Zumberge, J., Henry, M., Pollastro, R.M., 2007. Oil and gas geochemistry and petroleum systems of the Fort Worth Basin. AAPG Bull. 91 (4), 445–473.

Jing, W., Huiqing, L., Rongna, G., Aihong, K., Mi, Z., 2011. A new technology for the exploration of shale gas reservoirs. Pet. Sci. Technol. 29 (23), 2450–2459.

Kaufhold, S., Dohrmann, R., Klinkenberg, M., Siegesmund, S., Ufer, K., 2010. N_2-BET specific surface area of bentonites. J. Colloid Interface Sci. 349 (1), 275–282.

Keller, J.U., Staudt, R., 2004. Gas Adsorption Equilibria: Experimental Methods and Adsorptive Isotherms, first ed. Springer, New York.

Krooss, B.M., van Bergen, F., Gensterblum, Y., Siemons, N., Pagnier, H.J.M., David, P., 2002. High-pressure methane and carbon dioxide adsorption on dry and moisture-equilibrated Pennsylvanian coals. Int. J. Coal Geol. 51 (2), 69–92.

Langmuir, I., 1918. The adsorption of gases on plane surfaces of glass, mica and platinum. J. Am. Chem. Soc. 40 (9), 1361–1403.

Loucks, R.G., Reed, R.M., Ruppel, S.C., Jarvie, D.M., 2009. Morphology, genesis, and distribution of nanometer-scale pores in siliceous mudstones of the Mississippian Barnett shale. J. Sediment. Res. 79 (11–12), 848–861.

Lu, X.C., Li, F.C., Watson, A.T., 1995. Adsorption measurements in Devonian shales. Fuel 74 (4), 599–603.

Maes, N., Heylen, I., Cool, P., Vansant, E.F., 1997. The relation between the synthesis of pillared clays and their resulting porosity. Appl. Clay. Sci. 12 (1–2), 43–60.

Michot, L.J., Villieras, F., 2006. Surface area and porosity. In: Bergaya, F., Theng, B.K.G., Lagaly, G. (Eds.), Handbook of Clay Science. Dev. Clay Sci., vol. 1. Elsevier, Amsterdam, pp. 965–972.

Montgomery, S.L., Jarvie, D.M., Bowker, K.A., Pollastro, R.M., 2005. Mississippian Barnett Shale, Fort Worth basin, north-central Texas: gas-shale play with multi-trillion cubic foot potential. AAPG Bull. 89 (2), 155–175.

Noyan, H., Önal, M., Sarikaya, Y., 2006. The effect of heating on the surface area, porosity and surface acidity of a bentonite. Clay Clay Miner. 54 (3), 375–381.

Pierotti, R., Rouquerol, J., 1985. Reporting physisorption data for gas/solid systems with special reference to the determination of surface area and porosity. Pure Appl. Chem. 57 (4), 603–619.

Ross, D.J.K., Bustin, R.M., 2007. Shale gas potential of the Lower Jurassic Gordondale Member, northeastern British Columbia, Canada. Bull. Can. Petrol. Geol. 55 (1), 51–75.

Ross, D.J.K., Bustin, R.M., 2008. Characterizing the shale gas resource potential of Devonian–Mississippian strata in the Western Canada sedimentary basin: application of an integrated formation evaluation. AAPG Bull. 92 (1), 87–125.

Ross, D.J.K., Bustin, R.M., 2009. The importance of shale composition and pore structure upon gas storage potential of shale gas reservoirs. Mar. Petrol. Geol. 26 (6), 916–927.

Schettler, P., Parmoly, C., 1990. The measurement of gas desorption isotherms for Devonian shale. Devonian Gas Shale Technology Review (GRI) 7 (1), 4–9.

Strapoc, D., Mastalerz, M., Schimmelmann, A., Drobniak, A., Hasenmueller, N.R., 2010. Geochemical constraints on the origin and volume of gas in the New Albany Shale (Devonian–Mississippian), eastern Illinois Basin. AAPG Bull. 94 (11), 1713–1740.

Sun, Y., Liu, C.M., Su, W., Zhou, Y.P., Zhou, L., 2009. Principles of methane adsorption and natural gas storage. Adsorption 15 (2), 133–137.

Suzuki, I., Kiuchi, H., Saitou, K., 1995. Direct determination of effective bet-area of Xe, Kr, and CH_4. J. Catal. 155 (1), 163–165.

Volzone, C., Ortiga, J., 2004. Influence of the exchangeable cations of montmorillonite on gas adsorptions. Process. Saf. Environ. 82 (2), 170–174.

Zhang, T., Ellis, G.S., Ruppel, S.C., Milliken, K., Yang, R., 2012. Effect of organic-matter type and thermal maturity on methane adsorption in shale-gas systems. Org. Geochem. 47, 120–131.